Integration of Scientific Echo Sounders with an Adaptable Autonomous Vehicle to Extend Our Understanding of Animals from the Surface to the Bathypelagic

Citation	Moline, M. A., Benoit-Bird, K., O'Gorman, D., & Robbins, I. C. (2015). Integration of Scientific Echo Sounders with an Adaptable Autonomous Vehicle to Extend Our Understanding of Animals from the Surface to the Bathypelagic. Journal of Atmospheric and Oceanic Technology, 32(11), 2173-2186. doi:10.1175/JTECH-D-15-0035.1
DOI	10.1175/JTECH-D-15-0035.1
Publisher	American Meteorological Society
Version	Version of Record
Terms of Use	http://cdss.library.oregonstate.edu/sa-termsofuse

Integration of Scientific Echo Sounders with an Adaptable Autonomous Vehicle to Extend Our Understanding of Animals from the Surface to the Bathypelagic

MARK A. MOLINE

School of Marine Science and Policy, University of Delaware, Lewes, Delaware

KELLY BENOIT-BIRD AND DAVID O'GORMAN

College of Earth, Ocean, and Atmospheric Sciences, Oregon State University, Corvallis, Oregon

IAN C. ROBBINS

Center for Coastal Marine Sciences, California State Polytechnic University, San Luis Obispo, California

(Manuscript received 16 February 2015, in final form 7 August 2015)

ABSTRACT

Acoustic echo sounders designed to map and discriminate organisms in the water column have primarily been deployed on ships. Because of acoustic attenuation of higher frequencies used to detect and discriminate micronekton and nekton, this has effectively restricted the range of this information to the upper water column. In an effort to overcome these range limitations by reducing the distance between the transducer and the targets of interest, dual-frequency (38 and 120 kHz) split-beam echo sounders were integrated into a Remote Environmental Monitoring Units (REMUS) 600 autonomous underwater vehicle (AUV), effectively doubling the range of quantitative acoustic data into the mesopelagic zone (600–1200 m). Data from the first set of missions in a range of conditions revealed that the AUV provided a stable platform for the echo sounders and improved vertical and horizontal positional accuracy over echo sounders towed by ships. In comparison to hull-mounted echo sounders, elimination of ship noise and surface bubbles provided a 17- and 19-dBW decrease in the noise floor for the 38- and 120-kHz echo sounders, respectively, effectively increasing the sampling range by 30%–40%. The extended depth range also increased the resolution of the acoustic horizontal footprint from 37–40 to 0.6–3.7 m, enabling discrimination of individual targets at depth. Also developed here is novel onboard echo sounder data processing and autonomy to allow sampling not feasible in a surface ship or towed configuration. Taken together, these data demonstrate an effective new tool for examining the biology of animals in the mesopelagic zone (600–1200 m) in ways previously only possible in the upper ocean.

1. Introduction

While there have been continual advances in design, hardware, control software, navigation, and power management of propeller-driven autonomous underwater vehicles (AUVs), only in the last decade have they become common tools for industry (e.g., survey and environmental monitoring; George et al. 2002; Niu et al. 2009) and scientific investigation (Dickey et al. 2008). These systems occupy a unique time–space domain and increase our efficiency and capacity for measurement of oceanic environments (Yuh et al. 2011). One of the persistent challenges in applying AUV platforms has been the trade-off of size and power. The trend for many underwater technologies has been to miniaturize, which reduces logistic effort and cost but at the same time limits the mission duration and most importantly the sensor payloads. Most of AUVs currently in service have payloads for measurement and mapping of geophysical features, such as seafloor bathymetry, substrate type, and water velocity. Even though AUVs are ideal platforms to measure on scales relevant to biological systems, only a few have been instrumented for this purpose. Examples of such platforms include algal biomass, including harmful

Denotes Open Access content.

Corresponding author address: Mark A. Moline, School of Marine Science and Policy, University of Delaware, 700 Pilottown Rd., Lewes, DE 19958.
E-mail: mmoline@udel.edu

DOI: 10.1175/JTECH-D-15-0035.1

algae (Robbins et al. 2006), tracking of animal-borne pinging tags (Oliver et al. 2013), bioluminescence (Moline et al. 2005), and direct imaging (Barrett et al. 2010). Many of these measurements are based on optical sensors, which have gone through a revolution in miniaturization of both the active sources [e.g., light-emitting diodes (LEDs)] and detectors [e.g., silicon diodes and photomultiplier tubes (PMTs)]. Individual animal tracking is based on relatively high-frequency acoustics and short range and thus are also small. Because of this, these sensors have readily been integrated into small vehicles, such as the Remote Environmental Monitoring Units (REMUS) 100 (Moline et al. 2005), and investigating these biological phenomena have all been restricted by the vehicle type to the upper 100 m of the ocean with durations of <12 h. While revealing important aspects of biology and coupling to the physical environment, there is a significant fraction of the food web that cannot be measured with these sensor systems, from zooplankton to fishes, birds, and marine mammals.

Light in seawater is attenuated rapidly at visible wavelengths (Munk and Baggeroer 1994), making obtaining information on animals over large volumes of water challenging. Alternatively, sound in the ocean travels fast and efficiently with detection possible over relatively great distances. As a result, active acoustic techniques, those that use sounds that are both transmitted and received (e.g., sonars), are widely applied to fish, zooplankton, and other animals in the ocean for both fisheries and ecological studies (MacLennan and Holliday 1996). One of the key challenges for utilizing acoustics to study biology is the difficulty in identifying the source of the scattering (McClatchie et al. 2000). Because the frequency response of acoustic scattering from animals is affected by a combination of their size and material properties, the combination of multiple, discrete acoustic frequencies can aid interpretation (Holliday 1977). However, propagation losses increase with increasing frequencies, limiting the effective range of multifrequency acoustic techniques to the range of the highest frequency utilized. In addition to increasing signal loss with range, the effects of ship motion (Stanton 1982) and the beamwidth or footprint of the echo sounders increase with range.

One solution to overcoming the range limits of high-frequency echo sounders along with the lower quality and resolution of echo sounder data at depth is to reduce the range between the transducer and the targets of interest. Kloser (1996) accomplished this by using a deep-towed platform, conducting acoustic surveys from a depth of 600 m. While this approach provided insights into the seafloor-associated fish, the lengthy cables required present challenges in signal transmission, deployment, and navigation. AUVs have the potential to be much more efficient and capable deep-water platforms for echo sounders (Fernandes et al. 2003). Active acoustics are regularly integrated into autonomous platforms of all sizes for current measurement of water velocity and direction; the backscatter recorded as a diagnostic feature of acoustic Doppler current profiler measurements has been utilized to qualitatively describe the distribution of animals in the water column from autonomous platforms (Baumgartner and Fratantoni 2008). Previous efforts have provided major breakthroughs in integrating relatively large, power-hungry scientific echo sounders into AUVs, with three different vehicles adapted as platforms for quantitative echo sounders: Autosub (Griffiths et al. 2001), Hugin (Patel et al. 2004), and Explorer 3000 (Scalabrin et al. 2009). These platforms have provided information on vessel avoidance not possible from the vessels themselves (Brierley et al. 2003; Fernandes et al. 2000; Patel et al. 2004), acoustic data in the surface and bottom "blind zones" inherent in ship-based surveys (Brierley and Fernandes 2001; Scalabrin et al. 2009), and mapped biology in the water column beneath ice in the Antarctic without disturbing the ice substrate (Brierley et al. 2002). As these platforms and their acoustic payloads have evolved, they have revealed important aspects of the biology of krill, fish, and seabirds. However, because of the significant challenges in development and deployment, the gains promised by acoustic data acquired from autonomous platforms have not been fully realized. Our objective was to build on these previous developments and exploit the capabilities of an AUV to obtain dual-frequency (38 and 120 kHz), quantitative, split-beam (7° beamwidth) echo sounder data beyond the range effectively sampled simultaneously by both frequencies using shipboard sensors (<600 m) in order to explore biology in the mesopelagic zone (400–1000 m).

2. Sensor–platform integration

a. Vehicle description

In selecting an AUV platform ideal for the echo sounder application, it was essential to optimize the following capabilities: 1) operational depths of the vehicle needed to be at or beyond the effective multifrequency surface range of ship-mounted echo sounders (500–600 m); 2) a vehicle with sufficient power to both sustain a significant range/duration and power the transducers and associated computers necessary for onboard data acquisition and processing; and 3) the vehicle needed to both accommodate the relatively large diameter of a narrow-beam 38-kHz transducer (48 cm) and be as small as possible for logistical ease in deployment and recovery. A host of propeller-driven AUVs exist, and this diversity is largely driven by the current battery power densities and

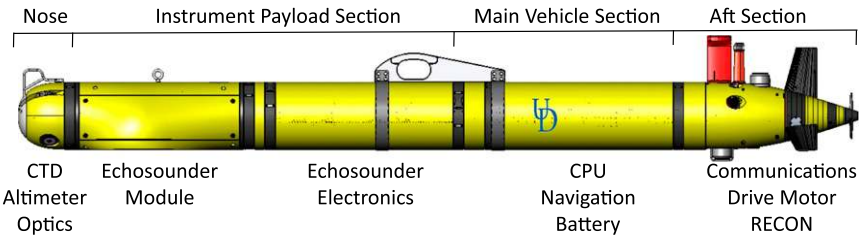

FIG. 1. The REMUS 600 vehicle with a specialized Simrad EK60 echo sounder payload section. The integrated vehicle includes an aft section, main vehicle section, the two echo sounder modules, and an instrumented nose section. The large red mast in the aft section is for Iridium, wireless, and GPS communications. The cylinders below and behind the mast are acoustic transponders for ranging and modem communications. Vehicle length in this configuration is 4.25 m.

duration requirements for a given application (see www.auvac.org). Larger vehicles tend to have both the depth tolerances beyond 600 m and the power requirements for longer-range capabilities. Fernandes et al. (2003) provides a comprehensive list of AUVs, their sizes, and respective ranges. Some of the largest vehicles with weights exceeding 2 t—such as Altec, Autosub, and Theseus—stand out from a range performance perspective with capabilities on the order of 600–1000 km, all are capable of operating below 600 m, and are sufficiently large to accommodate the acoustical sensors. Despite advances in battery technology since 2003, the ranges of AUVs have not significantly changed, highlighting the influence of higher-demand sensor payloads. In contrast to these larger systems, the REMUS 600 introduced in 2005 weighs only 250 kg with dimensions of 3.25 m × 0.3 m diameter. It has an operational depth of 600 m, with a range (400 km) and duration (70 h with a standard payload) comparable to the much larger Autosub and Theseus (Stokey et al. 2005b). Other midsized AUVs, such as the Bluefin-12 and Hugin, possess the required depth capabilities but have about half the range/duration capacity (Fernandes et al. 2003).

The REMUS 600 platform is largely based on the widely used REMUS 100 system (Moline et al. 2005). The REMUS 600 is designed as a series of hull sections that may be easily separated for reconfiguration, integration of new sensors, maintenance, or shipping. The REMUS 600 vehicle sections mechanically mate using a common clamping ring assembly that was derived from the well-proven MK 46 torpedo hull connection joint (Stokey et al. 2005b). Besides the hull construction, the most significant design difference between the REMUS 100 and the REMUS 600 vehicle is the aft section, which integrates the drive components, the control systems, and the communications (Fig. 1). The REMUS 600 has an oil-filled direct drive dc brushless motor connected to an open two-bladed propeller. The control surfaces are three fins in inverted "Y" configurations. The highly responsive fins allow the vehicle to control pitch, roll, and yaw, with alignment and stability—essential for optimizing the performance of a scientific echo sounder. The REMUS 600 has a number of modes of communication. While on the surface, the vehicle can communicate via an 802.11b "Wi-Fi" 2.4-GHz wireless networking system and via Iridium. This Wi-Fi allows for both navigation and high bandwidth, true-networked communications to all internal networked systems, and often eliminates the need to recover the vehicle between missions. The Iridium modem is optimal for emergency communications, routine status messages, and mission redirect commands. The Wi-Fi, Iridium, and Wide Area Augmentation System (WAAS)–GPS are integrated into the aft antennas. While the vehicle is subsurface, the REMUS vehicle interface program (VIP) on the surface can be in continuous communication with the vehicle via the 10-kHz acoustic modem, when the monitoring platform is within 4 km of the vehicle. The micromodem supports the latest version of the Compact Control Language (Stokey et al. 2005a). The modem uplink messages provide the vehicle's position, along with all critical system status, and provide the ability to send commands to the vehicle to interrupt its mission in progress, execute an alternate mission, or terminate the mission. In addition to the acoustic modem, there is a 4-kHz transponder on board for tracking with an effective range of up to 5 km under sea state conditions $<$ 2 m. The aft section also houses a secondary vehicle computer (RECON), which acts as a backseat driver, altering the vehicle's response to sensor input (see section 2c).

The main vehicle section forward of the aft section houses the vehicle's motherboard and battery trays containing 5200 Wh of rechargeable lithium-ion batteries (Fig. 1). Each battery tray contains electronics for monitoring and controlling charge and discharge, cell balancing, capacity metering, and safety systems. In the configuration for the science echo sounder, only the one battery tray in this section was used; however, a second section with two additional battery sections could be added for an additional 10 400 Wh of power. Charging is

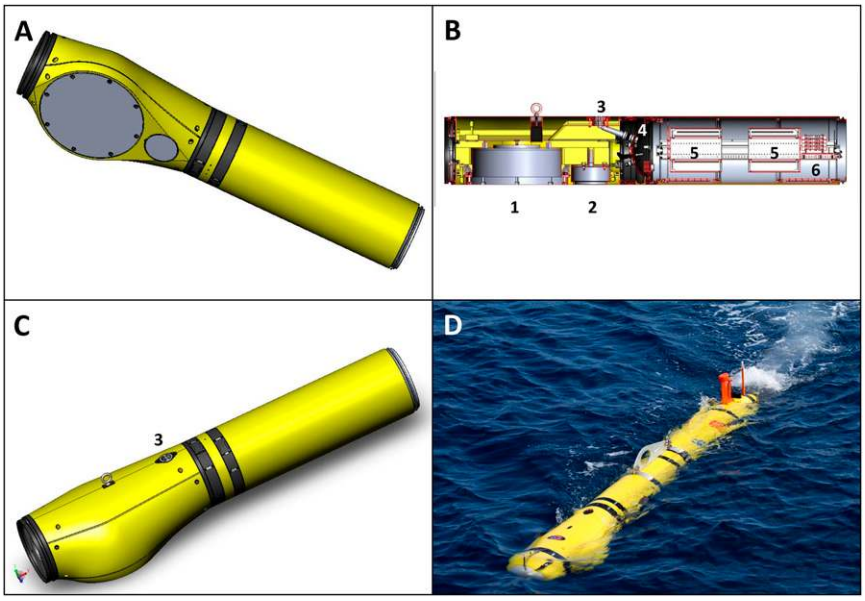

FIG. 2. The two Simrad EK60 echo sounder modules. (a) View from underneath the instrument modules showing the larger 38-kHz and smaller 120-kHz transducers in the forward module. This module is flooded with a bulkhead separating the aft electronics module. (b) An internal side view of the echo sounder payload with the 1) 38- and 2) 120-kHz transducers, 3) wired Ethernet access port, 4) bulkhead, 5) EK60 GPTs, and 6) dual PC/104 stack. The aft module is open to the main vehicle section in Fig. 1. (c) Top view of module showing the form factor accommodating the large transducer and the port for the Ethernet connection as in (b). (d) Integrated vehicle underway beginning a mission off Southern California.

accomplished through a shore power connection, requiring only a simple commercial 32-Vdc power supply. Charging may be done without opening or ventilating the housing, due to the zero outgassing properties of the lithium-ion (Li-ion) cells. The batteries may be fully charged from a residual charge of 20% in less than 12 h.

The scientific echo sounders and control/processing computers were integrated into two sections (described below) forward of the main vehicle section, with a nose section forward of the bulkhead (Fig. 1). The nose houses additional sensors, including a Neil Brown Ocean Sensors, Inc., glider CTD (G-CTD) (Schmitt and Petitt 2006); two Wet Labs Inc. Environmental Characterization Optics (ECO) pucks for measurement of chlorophyll a, colored dissolved organic material, and backscattering (Moline et al. 2010). An Imagenix 863 pencil-beam altimeter (Zawada et al. 2008) was also incorporated into the nose and networked to the navigation system for terrain following and avoiding bottom collisions.

The VIP allows the operator to plan a number of mission types based on depth, altitude, and horizontal location (see Moline et al. 2005). Although there are many modes of operation for the REMUS platform, because of the need for vehicle stability in this application, constant depth mode was most commonly employed. Navigation of the vehicle was solely based on an onboard compass and corrections were made by intermittent GPS corrections on the surface. The surface positions were used to renavigate the underwater portion of the mission. Typical surfacing intervals were between 2 and 5 h with horizontal offsets between 20 and 500 m from the intended location, dependent on advective flow at the vehicle (see Moline et al. 2005). This works out to between 0.06% and 1.6% drift as a function of distance traveled, which is slightly higher than inertial navigation systems that have been measured at 0.1% for long-duration missions such as the ones in this study (Panish and Taylor 2011).

b. *Echo sounder integration*

Two off-the-shelf Simrad EK60 (Andersen 2001) general-purpose transceivers (GPTs) (38 and 120 kHz) were modified to fit inside the dry payload bay of the REMUS (Fig. 2a). The electronic cards on each transceiver are typically connected through a backplane that arranges the cards linearly. However, the longest dimension of the standard backplane exceeds the interior diameter of the vehicle's payload bay. We used custom backplane boards that arranged the electronics cards in an X shape to decrease their diameter. Each modified GPT is surrounded by a custom-built enclosure that allows it to mount to rails that slide into the standard REMUS guide system (Fig. 2b). These transceivers are

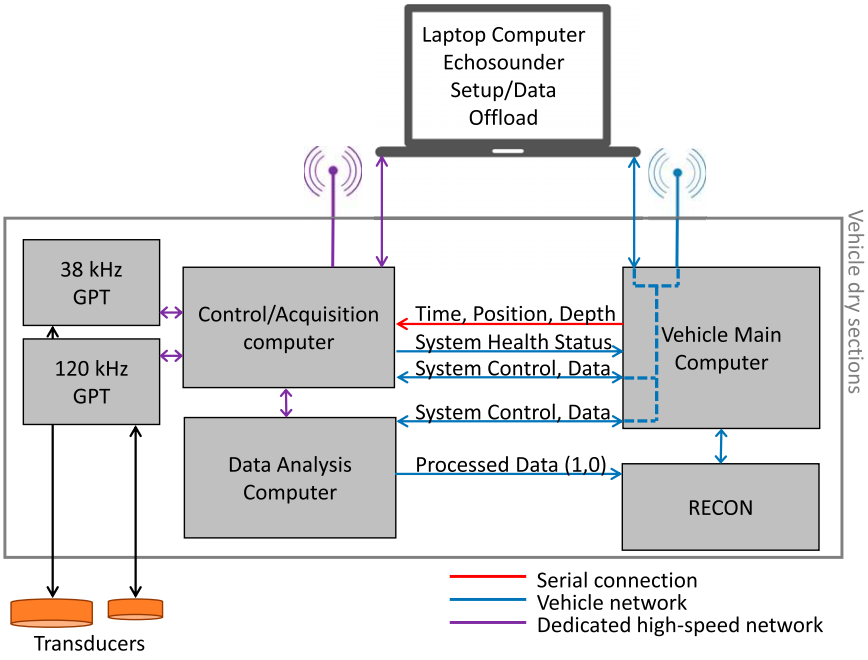

FIG. 3. Block diagram of vehicle connections among the four computers and two echo sounder systems inside the AUV, as well as an external laptop for setting up the system and offloading data. Connections are indicated by lines with arrows showing the direction of data flow. Dotted lines indicate pass through of information. Connections include a serial link (red) that provides vehicle data to the echo sounder data acquisition computer for synching with the data stream, the vehicle's Ethernet network (blue), and a secondary, high-speed Ethernet dedicated to the echo sounder system (purple).

connected through a watertight bulkhead to 1500-m-depth-rated 7° beam echo sounder transducers (Simrad ES120-7CD with a diameter of 18 cm; Simrad ES38DD with a diameter of 48 cm) mounted in a wet payload bay, forward of the electronics payload (Fig. 2b). The housings and mounts for the EK60 general-purpose transceivers were designed to allow the GPT electronics to be grounded while being isolated from the REMUS hull to allow for isolation from electrical noise and the electrically driven REMUS hull that serves as part of the REMUS leak detection system. Additionally, we undertook extensive measurements in the laboratory and preliminary deployments to identify and mitigate sources of noise in the AUV system prior to field experiments, for example, adjusting the switching frequency of the AUV's drive motor, shielding cables, installing filters on power lines, modifying internal grounding paths, isolating electronics, and altering cable positions.

The echo sounder transceivers were connected via Ethernet to two PC/104 form-factor computer stacks attached to the same rails as the transceivers using custom mounts and adapter plates (Fig. 2b). Each computer stack is a VersaLogic Leopard–based 2.26-GHz commercial temperature Intel Core 2 Duo processor with 4-GB RAM, dual gigabit Ethernet, and two solid-state hard drives running the Windows 7 operating system. Both computers are coupled to the vehicle's network via Ethernet, allowing the computers to be viewed and controlled remotely through the vehicle's wired and wireless connections. The computers are also connected to a separate gigabit Ethernet system with a dedicated wireless antenna and a wired port to facilitate the rapid transfer of the extensive datasets that can be acquired by the echo sounders (Figs. 2b,c). One computer stack runs Simrad's ER60 data acquisition software along with the operating system on one hard drive and acquires data directly to its second hard drive (Fig. 3). This computer stack also has a serial connection to the vehicle computer that provides time, vehicle depth, and pseudo-GPS position that is automatically merged into the acoustic data stream utilizing existing navigation input options within the ER60 software.

c. Data processing and autonomy

The second computer stack in the dry payload bay is responsible for processing data and providing synthesized results to the vehicle to modify navigation. As processing the echo sounder data is computationally demanding, separation of data acquisition and data processing ensures the robustness of the system. The processing computer runs Echoview software (Echoview Software Pty Ltd,

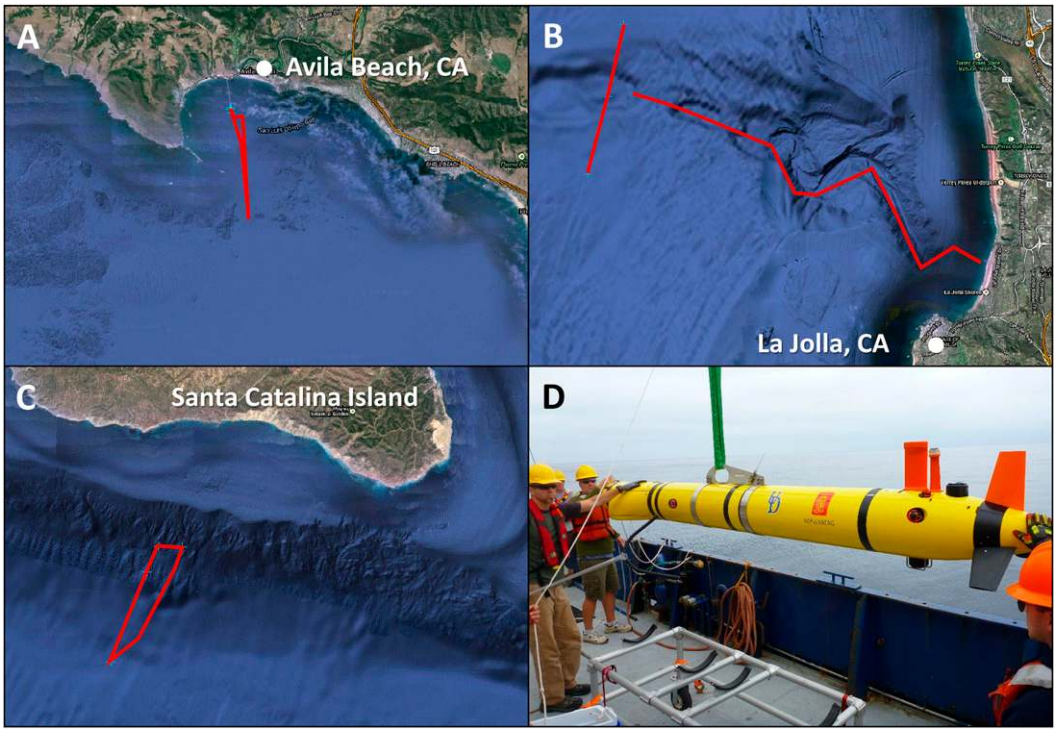

FIG. 4. REMUS 600 missions demonstrating the technology. (a) Test 1, shallow transect in San Luis Obispo Bay. Mission length of 16 km. (b) Missions off La Jolla. Mission on east side was test 2, a 15-km transect out to Soquel Canyon. The western 5-km transect was mission A, part of the primary study examining abundance and distribution of deep prey fields. (c) Mission D off the shelf break south of Santa Catalina Island. Mission length was 10 km. (d) Deployment of integrated REMUS 600 for mission D. After the vehicle was released, it was driven away manually from the vessel via wireless and then sent the command to start the mission. On return, the vehicle would be driven manually back to the side of the ship for pick up.

Hobart, Tasmania, Australia) as well as a custom stand-alone Windows-based application written in C++ that manages the software by shutting it down and restarting it hourly and passes processed information to the vehicle's computer via Ethernet at the frequency determined within the data processing program implemented within Echoview. This architecture was chosen because Echoview has numerous tools available for application to these data, it has been optimized for memory management on these large datasets, it provides consistency with the postcruise processing approaches we apply to the acoustic data, and it allows the data analysis approach to be changed between missions or projects as the science goals for the vehicle change. Echoview is a standard tool for the analysis of echo sounder data and, in "Live Viewing" mode, provides robust near-real-time analysis that can incorporate basic data processing (removal of the seafloor, correcting data depth as the vehicle dives, removal of noise, etc.) along with tools for combining the two frequencies of acoustic data, analysis of solitary targets, volume scattering integration, and more. These analyses are incorporated into a visually programmed "data flow" that is saved as a distinct file that can easily be replaced as analysis needs within the vehicle change. Of critical importance to the autonomous operation here, our data processing flow resulting in the flagging of each individual pixel in the dataset as of interest or not (1 or 0, respectively) based on the scattering characteristics of biological targets of interest. For our test deployments, these were then summed over the water column below the vehicle (up to 600 m) every 30 s. If the sum of these positive hits exceeded the threshold determined within the data flow, then the custom application running on the stack sent a "1" to the vehicle's RECON computer; otherwise, it sent a zero. A 1 or 0 flag was encapsulated and transmitted as a User Datagram Protocol (UDP) data packet through the vehicle network (Fig. 3). These outputs occurred within 30 s of the acquisition of the data, providing close to real-time feedback to the vehicle. The RECON computer was programmed to respond when the UDP data packet sends a "1," taking over the primary navigation from the vehicle's motherboard, pausing the primary mission, and executing a secondary mission for either a set amount of time or until additional sensor input met some prescribed

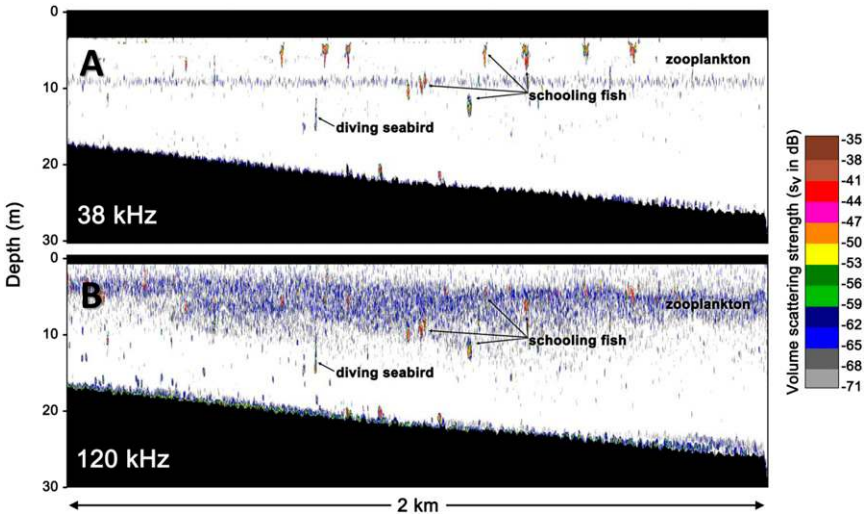

FIG. 5. Echograms from the (a) 38- and (b) 120-kHz echo sounders for a 2-km portion of test 1 (see Fig. 4a). This initial deployment indicates the importance of using more than one frequency to aid in the classification of biological targets. During this mission, diving seabirds were visually observed at the surface. As in previous work (Benoit-Bird et al. 2011), echoes from a stream of bubbles leaving the plumage of a diving bird are clearly visible at both frequencies utilized. Similarly, schools of fish are detected at both frequencies, while zooplankton are visible only at 120 kHz.

condition. In testing this autonomous application, we set a threshold for one target class based on dual-frequency backscatter properties and overall intensity with a vehicle response to increase the spatial resolution of sampling around the location where the positive signal was received by modifying the vehicle's path. After 20 min the RECON computer would then transfer the vehicle navigation back to the primary CPU and continue its primary preprogrammed mission.

3. Instrument validation

a. Introduction

To validate the performance of the newly integrated AUV system, we developed a series of open ocean tests. Each sequential test was designed to build on the previous effort in evaluating the performance of both the vehicle and echo sounders. Here, we draw on the two test missions and two primary missions to illustrate the function and innovation of the platform. In all tests, the echo sounders used a 1.024-ms-long pulse (input power: 1000 W at 38 kHz and 500 W at 120 kHz). Testing for this system occurred on the U.S. West Coast and began with a shallow-water test in San Luis Obispo Bay, California, in July 2012 (Fig. 4a). This mission followed a 4-km offshore transect, returning to shore and repeating. The mission was in depth mode operating at 4 m, designed to evaluate the basic function of the echo sounders (Fig. 5) and the stability of the AUV platform. The second test in April 2013 was a deep mission off of

TABLE 1. REMUS 600 flight performance metrics for the two initial test missions and two of the primary missions (MSN), MSN A and MSN D (see Fig. 4). Test 1 was performed over 16 km off of San Luis Obispo Bay at 4 m, and test 2 was performed off La Jolla. Test 2 was flown at 10 m but included a deep segment over Soquel Canyon at 300 m. Mission A was flown at 50-m transverse to the western end line of test 2. Mission D was flown at three target depths over the shelf break off the south coast of Catalina Island on 19 Sep 2013. Included are mean values ($\pm\sigma$) of measured vehicle depth, pitch, and roll, and the difference in heading between measured and goal. The vehicle's programmed goal for pitch, roll, and heading difference are all 0°.

	Goal (m)	Depth (m)	Pitch (°)	Roll (°)	ΔHeading (°)
Test 1	4	3.97 ± 0.07	−0.90 ± 0.84	−0.10 ± 0.72	−0.01 ± 0.70
Test 2	10	9.98 ± 0.08	−0.47 ± 0.49	−0.14 ± 0.75	−0.35 ± 10.16
Test 2	300	299.99 ± 0.05	−0.70 ± 0.63	−0.27 ± 0.64	−0.44 ± 8.26
MSN A	50	49.98 ± 0.07	0.09 ± 0.42	0.05 ± 0.35	0.02 ± 0.14
MSN D	50	49.98 ± 0.04	0.42 ± 0.27	0.02 ± 0.21	0.02 ± 0.16
MSN D	300	299.98 ± 0.03	0.78 ± 0.30	0.10 ± 0.33	0.00 ± 0.16
MSN D	500	499.99 ± 0.03	0.79 ± 0.21	0.03 ± 0.20	0.02 ± 0.11

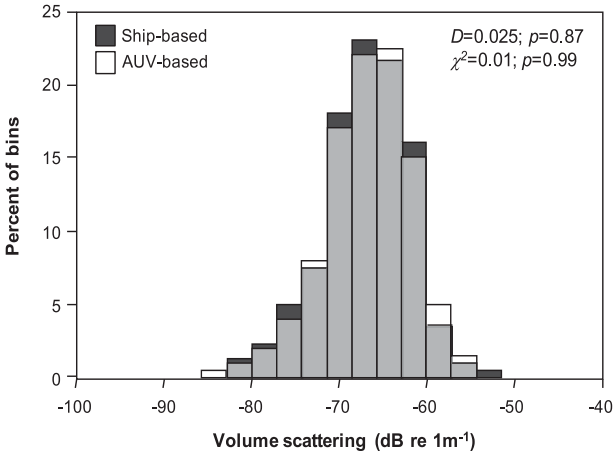

FIG. 6. The distribution of volume scattering strength at 38 kHz between 500 and 1000 m measured from the ship (black bars) and the AUV at a dive depth of 500 m (white bars) for a 5-km-long portion of mission D (see Fig. 4c). Regions of overlap between the two distributions are shown in gray. There were no significant differences in the mean or distribution of the two datasets.

Scripps Pier in La Jolla, California, and was designed to fly over Soquel Canyon to evaluate the acoustic range of the echo sounders and to operate in deeper waters (Fig. 4b). The mission profile was to navigate offshore 10 km at 10 m and then dive to 300 m over the canyon. These tests led to the first intended application of the vehicle along the Southern California coast (Fig. 4b) and in the deep canyons in the Channel Islands between Santa Catalina Island and San Clemente Island (Figs. 4c,d). These primary missions occurred in September/October 2013 with the goal to measure the distribution and abundance of deep-water prey fields (i.e., krill, fish, and squid) in this area to understand how prey affects the behavior of deep-diving whales. This is the first time mesopelagic depths have been evaluated for these sound scattering prey using an AUV.

b. *Vehicle performance*

While the REMUS 600 is known to perform well in a range of environmental conditions (Stokey et al. 2005a), it was important to fully evaluate the flight characteristics of the new vehicle form factor, particularly in light of how the section faired around the large, low-frequency transducer near the nose (Figs. 2c,d), for the deep echo sounder application. In both the "shallow" and "deep" water tests, the vehicle conducted the missions as planned. Flight metrics show that the vehicle achieved depth fidelity, heading—and important for the acoustic application—level flight (Table 1). This was consistent between missions and at different depths within a given mission, which would have not been possible for a ship-towed configuration (Kloser (1996). In the both the testing phase and the implementation phase in the Channel Islands, the vehicle offset from the planned track was not a serious issue, with navigation easily corrected based on GPS positions. For example, a mission conducted on 29 September traveled 30 km without surfacing with a total offset from the planned endpoint of 200 m, less than a 0.7% cumulative error. The REMUS 600 typically has an inertial navigation system for increased positional accuracy; however, it was not needed for this open ocean application. The ship was often in direct contact with the vehicle for updated progress in a given mission. For the deep application of this platform, it was important to rapidly transit to the prescribed depth to begin measurement. In addition to setting a depth heading, the VIP has a DRIVE DESCENT command that increases the downward pitch, effectively decreasing the time interval to set depth (30 m min^{-1}). The vehicle does not, however, have a concomitant DRIVE ASCENT command, so the time to surface (although an active command to SURFACE) took approximately twice as long. This needed to be considered in mission objectives and planning. For the primary effort between 17 September and 1 October 2013, the vehicle performed 28 missions, traveling over 650 km with the longest mission time of ~17 h. The platform was robust, with a straightforward deployment and recovery protocol (Fig. 4d).

c. *Echo sounder performance*

The echo sounders performed as designed with full control of power and software through both the vehicle and the dedicated wired and wireless networks. This allowed rapid offloading of data and control of the settings of the echo sounder. In practice, the vehicle's wireless network connection allowed us to communicate with the echo sounder acquisition and processing computers up to ~50 m from vehicle when it was at the surface of the water. This allowed us to change the echo

TABLE 2. The mode noise level (dBW) measured from the AUV and from the ship under two different weather conditions: calm, when seas were glassy with no whitecaps; and moderate, where small to moderate waves often had whitecaps. The 95% confidence interval is shown in parentheses for each measurement.

	AUV	Ship—Calm	Ship—Moderate
38 kHz	−161 (−163 to −159)	−144 (−148 to −134)	−140 (−143 to −128)
120 kHz	−158 (−160 to −155)	−139 (−132 to −126)	−137 (–133 to −125)

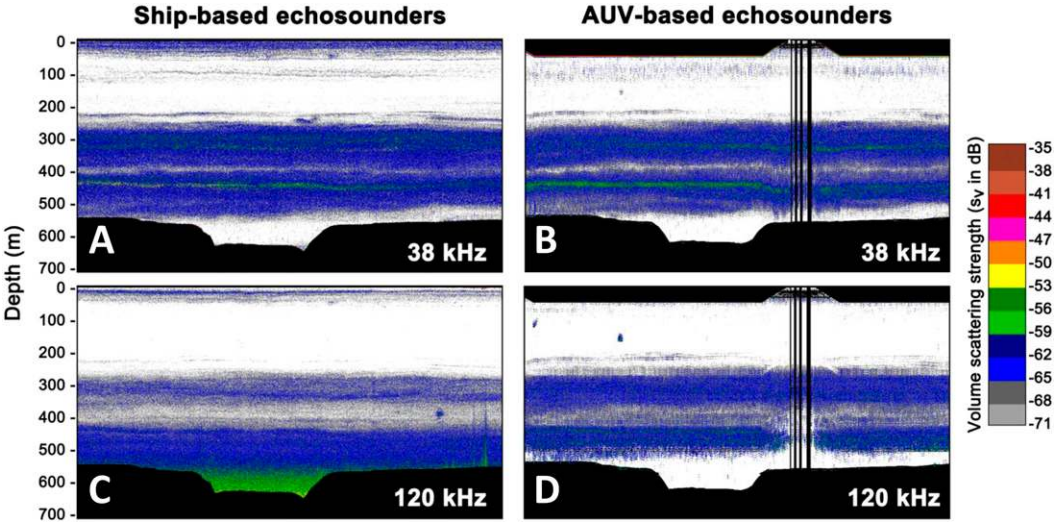

FIG. 7. A 10-km-long echogram from mission A (see Fig. 4b) surveyed by both (a),(c) the ship and (b),(d) the AUV at 38 kHz and 120 kHz off La Jolla. The AUV sampled from a depth of 50 m with a surfacing near the middle of the transect. Both datasets show true depth to allow easy comparison. Data from below the seafloor, areas of acoustic ring down near the transducers, and some regions of bubble-induced data washouts when the AUV was at the surface are shown in black. Background noise, however, is not removed. The volume scattering strengths measured are not significantly different between platforms throughout the overlapping effective ranges of each echo sounder. However, one important thing to note is the area of yellow and green scattering near the depression in the seafloor in the 120-kHz data from the ship that is missing from the AUV-based data. This monotonically increasing scattering is caused by amplification of noise by the time-varying gain of the echo sounder. The lower noise floor in the AUV-based echo sounder shows the effective range of the AUV-based echo sounder is larger than the ship-based system under typical conditions.

sounder settings to run noise tests, start and stop pinging while the vehicle was in the water in order to limit the potential of damage to the transducers, and to run the software's calibration protocol much like we would on shipboard sensors.

1) CALIBRATION

To calibrate the echo sounders inside the AUV, we employed two approaches. First, we employed a standard sphere method (Foote et al. 1987) to calibrate the echo sounders at the surface, tethering the AUV to the side of the research vessel while running the ER60 calibration routines. To validate the AUV echo sounder calibrations at depth, we conducted ~5-km-long parallel surveys with the calibrated ship-based and AUV echo sounders over areas with extensive scattering layers using 1.024-ms-long pulses every 1.7 s. The AUV was held at a constant depth of 50, 300, or 500 m for each survey to allow for comparisons of volume scattering strength between the two platforms to be made over the diving depth range of the AUV. Volume scattering strength was calculated in 100-m-long × 50-m-deep bins to a depth of 1000 m for the 38-kHz echo sounder and to 400 m for the 120-kHz echo sounder. For bins that coincided in depth for both platforms, the distribution of volume scattering strengths for each transect were compared using Kolmogorov–Smirnov statistics, while mean values were compared using χ^2 tests.

Comparisons of acoustic scattering strengths measured with the ship-based and AUV-based echo sounders were conducted over a range of AUV dive depths. A sample of the distribution of depth-aligned 38-kHz volume scattering strengths measured along a single transect from the ship and the AUV at a dive depth of 500 m are shown in Fig. 6. The distributions of these two observations were not significantly different ($D = 0.025$, $p = 0.87$) nor were their means ($\chi^2 = 0.01$, $p = 0.99$). Over a total of 36 comparison transects, D ranged from 0.003 to 0.128 (p values: 0.99–0.33), while χ^2 ranged from 0.005–0.584 (p values: 0.99–0.51). There were no significant differences in the distribution of volume scattering or the mean value at either frequency or at any AUV dive depths ($n_{50m} = 8$, $n_{300m} = 13$, $n_{500m} = 15$). We conclude that the data from both echo sounders can be used quantitatively across the AUV's entire dive range. This is in contrast to prior calibrations of transducers over a range of pressures (e.g., Kloser 1996), suggesting the design choices made by the manufacturer in these transducers, which are marketed for deep-water applications, have been effective, at least to the dive depths the REMUS 600 is capable of achieving.

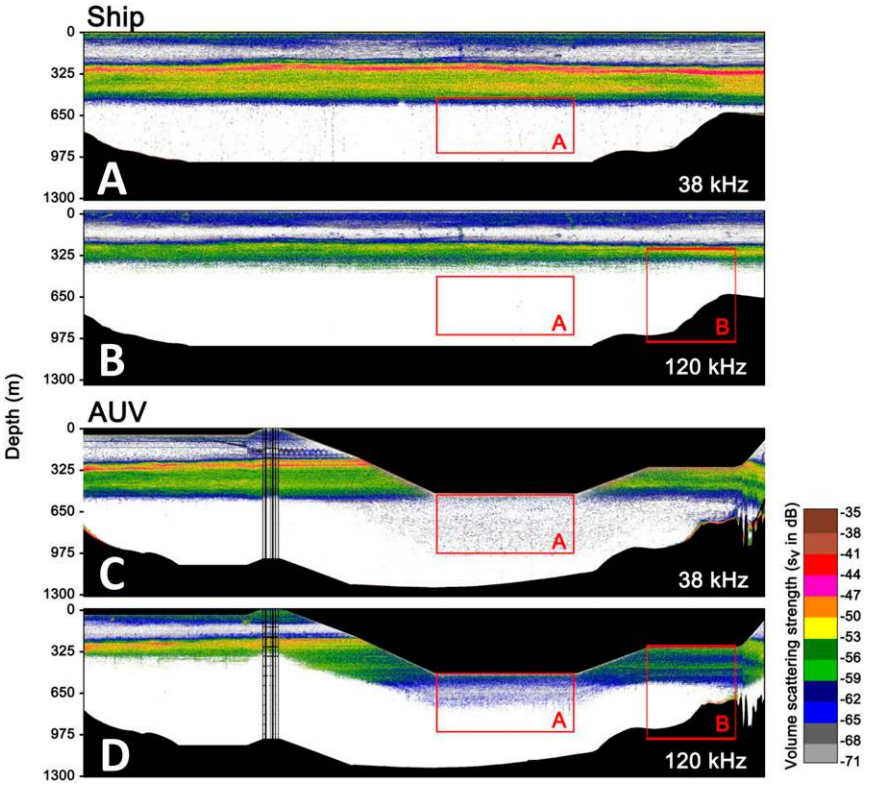

FIG. 8. Echograms from mission D (see Fig. 4c), a 10-km transects run in parallel by (a),(b) the ship and (c),(d) the AUV at 38 and 120 kHz in California's Catalina basin. The AUV sampled from a depth of 50 m, followed by a surfacing, then at depths of 500 and 300 m before surfacing again. Data from below the seafloor, areas of acoustic ring down near the transducers, and some regions of bubble-induced data washouts when the AUV was at the surface are shown in black. Data are processed here as is typical for acoustic surveys, removing background noise, resulting in the apparent loss of all but the strongest targets at great depths, particularly from the 120-kHz data. Details of these effects are shown for boxes A and B in Fig. 9.

2) SYSTEM NOISE

Baseline self-noise levels incorporating both electrical and acoustic noise of the ship-based and AUV-based echo sounders under typical deployment conditions were measured in deep water when the instruments were not pinging (e.g., were passively listening). The ship was operated at a speed of 5 kt (1 kt = 0.51 m s^{-1}), at the low end of the typical range used for ship-based surveys, using the propeller revolutions per minute and pitch determined to cause the least noise at that speed under two conditions: calm (almost no wind and flat seas) and moderate (light winds with scattered whitecaps). The AUV was sent on a standard mission to a depth of 20 m with light wind and scattered whitecap conditions but in listening-only mode (not pinging) to allow for measurement of noise using the onboard ER60 software. The ship carried the same 120-kHz transducer with a 7° beam but a smaller 38-kHz transducer with a 12° beam. The echo sounder's manual advises that noise measurements should be no higher than −145 dBW at 38 kHz and only modestly higher at higher frequencies. Results of 15 min of noise testing for each combination are shown in Table 2. The AUV echo sounders had a lower and more stable noise floor than the ship-based instruments even in the calmest seas. The AUV-based echo sounders had a 16- and 13-dBW advantage over the idealized noise floor of −145 dBW at 38 and 120 kHz, respectively. The advantage of the AUV-based data relative to data collected in the same experiment from a ship in calm conditions (e.g., no whitecaps visible) was 17 and 19 dBW at 38 and 120 kHz, respectively. From a practical perspective, this means that when a −75-dB threshold, a common choice, is applied to our volume scattering data, background noise is not detectable at 38 kHz to a range of 1530 m from the AUV sensors rather than 1140 m from the ship and 420 m from the AUV rather than 305 m from the ship at 120 kHz (Fig. 7). These ranges do not represent the limits of detection; but, they do provide a measure of the impact of noise on the

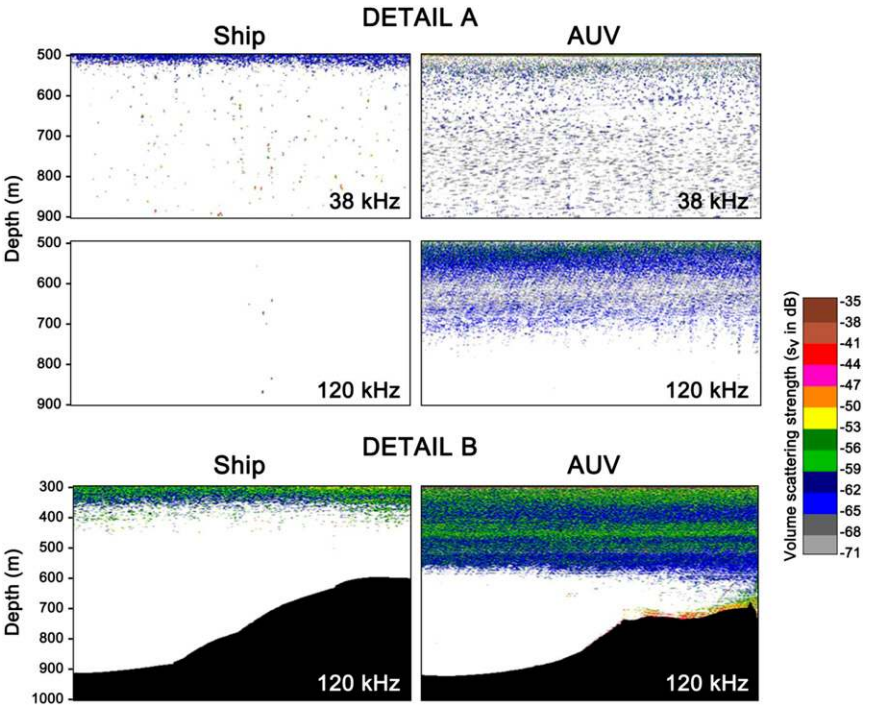

FIG. 9. Details of data from boxes A and B in Fig. 8 illustrate the effects of lowering the transducers on the detection of targets. (a) A diffuse layer of acoustic scattering is detectable at 120 kHz from the AUV but completely outside the range of the ship-based sensor. While a depth of 600 m is typically considered well within the effective range of the 38-kHz sensor, the AUV reveals numerous relatively weak solitary targets that are undetectable below the strong scattering layer detected by both systems. (b) Even at a depth of 350 m, the ship-based 120-kHz sensor fails to detect a moderately intense scattering layer that is clearly observed by the AUV-based sensor.

data quality. The low noise floor achieved within the AUV means that weaker targets can be isolated from noise at a given depth and, similarly, that the detection range for a given target is 30%–40% greater.

One feature of the acoustic data not noted in the table are the relatively frequent, high noise outliers that were present in the ship data and were completely absent from the AUV data. Further, noise measurements for the ship-based estimates were made under ideal ship conditions, which were frequently altered to deal with ship maneuvering, increasing the noise levels periodically and unpredictably. While the sources of each noise spike on the ship cannot be isolated, noise is often caused by other electronics, including wireless signals, imperfect power from generators, other scientific equipment, the engines, and variation in significant power draws on the vessel. While we used isolated batteries as a power supply and carefully grounded the instruments directly to seawater, it is nearly impossible to isolate these sources of noise on common use research vessels. Noise levels from AUV missions were stable once the AUV reached a depth of 5 m, regardless of maneuvering or changes in speed. This is largely because the AUV's sources of power and its draws are limited and remain relatively constant. The field testing reported here shows the effectiveness of the extensive efforts to identify and mitigate sources of noise in the AUV system prior to field experiments.

3) ACOUSTIC DATA QUALITY

Two other observations are important for examining the quality of the data obtained by the AUV echo sounders. First, bubbles are an important source of signal attenuation that was not captured by our passive noise examinations. The effects of bubbles were periodically apparent in the ship survey data. While we did not directly measure signal attenuation, at the wind speeds measured during the survey, it could have been 3 dB or more (Dalen and Lovik 1981), representing a signal loss of 50%. No effects of bubbles were detected in the AUV-based echo sounder data once the AUV dove below the upper few meters of the water column. Second, platform motion can be an important source of variation in the measurement of echo intensity. Based on the typical roll experienced on the ship during our

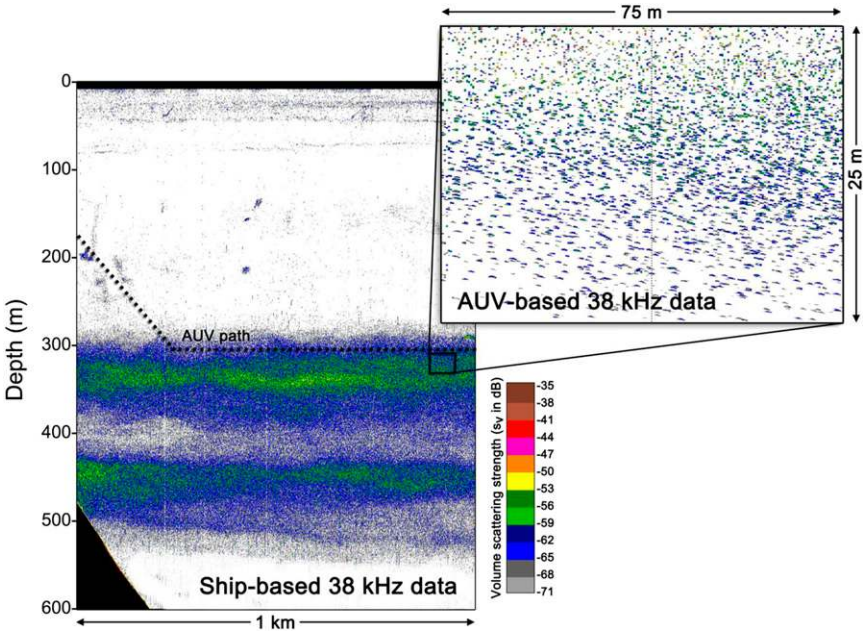

FIG. 10. Acoustic data collected from mission D at 300 m with both the ship-based (large panel) and AUV-based (inset) 38-kHz echo sounder illustrate the resolution gained by approaching targets within the scattering layer. The 75-m section from the AUV-based echo sounder represents just two beamwidths of the ship-based echo sounder. While these closely spaced scatterers can only be detected as a layer from the ship, the isolated crescent-shaped marks in the inset indicate that individual scatterers can be resolved with the AUV-based echo sounder, and thus it is possible to measure their target strength and the frequency response of individual targets in addition to measuring volume scattering from the entire layer.

cruise, echo intensity could vary by as much as 50% due to ship motion alone (Stanton 1982). As highlighted in Table 1, there was very little motion of the AUV during the level flight portion of any deployment and thus no changes in echo intensity are expected in the AUV data due to the platform itself.

4) ADVANTAGES GAINED BY DIVING ECHO SOUNDERS

The primary goal of this effort was to obtain data with the AUV at greater depths than is possible with ship-based sensors. The effects of this are evident when comparing ship-based and AUV-based data at the same depths but very different ranges (Figs. 8, 9). First, some organisms are observed with the AUV while diving that were not detectable from the ship, particularly those that are diffuse and weakly scattering but even some moderately intense and consistent scattering layers evident from the AUV are missing from the ship-based echo sounder data (Fig. 9). Second, even for scattering that is detected by echo sounders on both platforms, the resolution of the data is quite different. For example, Fig. 10 shows a scattering layer at a depth of just over 300 m measured from the surface with the ship and from a depth of 300 m from the AUV. At the range this feature is sampled, the ship-based sensor has a horizontal footprint of 37–40 m, while the AUV sensor has a footprint of 0.6–3.7 m. This increase in resolution means that instead of seeing a scattering layer, the AUV resolves scatterers individually. Using the split-beam characteristics of the echo sounder transducers, the absolute intensity of each scatterer can be measured and the frequency response of each individual quantified, making it possible to classify the scatterer into taxonomic categories and to estimate its length. Together, these advantages make it possible to examine the biology of animals in the mesopelagic zone in ways previously only possible in the upper ocean.

4. Conclusions

Data from the first set of missions in a range of conditions revealed that AUV-based echo sounders show increased performance in terms of effective range, thresholds of measurable volume scattering strength, and resolution of the targets relative to ship-based sampling. Even for the near-surface waters, the ability to fly the echo sounders close to the targets of interest allow for improved quantitative data on the distribution of organisms (i.e., acoustic scattering layers) and their behavior, such as diurnal vertical migrations. The AUV proved to

be an effective platform for these sensors, providing excellent depth stability, reduced noise, improved position information at depth, and versatility with respect to addressing both small- and large-scale sampling resolution through mission programing. While not emphasized here, the AUV carries additional sensor suites to associate the target organisms with their environment (i.e., physical/optical). Additionally, the integration of echo sounders into an AUV with the capability for autonomy allows for additional avenues of investigation, such as matching the sampling resolution to the critical horizontal and/or vertical length scales of the target field (see Deutschman et al. 1993), target tracking (i.e., marine mammals), and integrating with other sensor systems and networks. Quantification of animal dynamics (individuals to communities) over relevant time and space scales has largely been absent for the mesopelagic due to sampling limitations. Here, we demonstrate an integrated platform that will begin to provide answers for this zone of the ocean.

Acknowledgments. We thank our collaborator, Brandon Southall, for coordination and access to study areas. Excellent field support was provided by Chad Waluk, David Cade, Megan Cimino, Danielle Haulsee, Marnie Jo Zirbel, John Calambokidas, and Ari Friedlander. We thank Marnie Jo Zirbel for laboratory analysis. The captain and crew of the R/V *New Horizon* and staff of the SIO Nimitz Marine Facility are thanked for their efforts in supporting the AUV operations and target validation studies. Kongsberg Hydroid Inc., especially Chris von Alt, Kongsberg Simrad, and Jeff Condiotty, are thanked for their partnership in echo sounder integration into the AUV. Matthew Wilson, David Millington, Briony Hutton, and Toby Jarvis from Echoview were creative and supportive partners in developing the internal data analysis process. Funding was provided by the Strategic Environmental Research and Development Program (SERDP). We thank SERDP program manager John Hall for the encouragement and support, and we appreciate the guidance provided by the SERDP RC Technical Committee.

REFERENCES

Andersen, L. N., 2001: The new Simrad EK60 scientific echo sounder system. *J. Acoust. Soc. Amer.*, **109**, 2336, doi:10.1121/1.4744207.

Barrett, N., J. Seiler, T. Anderson, S. Williams, S. Nichol, and S. Hill, 2010: Using an autonomous underwater vehicle to inform management of biodiversity in shelf waters. *OCEANS 2010 IEEE—Sydney*, IEEE, 146–151.

Baumgartner, M. F., and D. M. Fratantoni, 2008: Diel periodicity in both sei whale vocalization rates and the vertical migration of their copepod prey observed from ocean gliders. *Limnol. Oceanogr.*, **53**, 2197–2209, doi:10.4319/lo.2008.53.5_part_2.2197.

Benoit-Bird, K. J., K. Kuletz, S. Heppell, N. Jones, and B. Hoover, 2011: Active acoustic examination of the diving behavior of murres foraging on patchy prey. *Mar. Ecol. Prog. Ser.*, **443**, 217–235, doi:10.3354/meps09408.

Brierley, A. S., and P. G. Fernandes, 2001: Diving depths of northern gannets: Acoustic observations of *Sula bassana* from an autonomous underwater vehicle. *Auk*, **118**, 529–534, doi:10.1642/0004-8038(2001)118[0529:DDONGA]2.0.CO;2.

——, and Coauthors, 2002: Antarctic krill under sea ice: Elevated abundance in a narrow band just south of ice edge. *Science*, **295**, 1890–1892, doi:10.1126/science.1068574.

——, and Coauthors, 2003: An investigation of avoidance by Antarctic krill of RRS *James Clark Ross* using the *Autosub-2* autonomous underwater vehicle. *Fish. Res.*, **60**, 569–576, doi:10.1016/S0165-7836(02)00144-3.

Dalen, J., and A. Lovik, 1981: The influence of wind-induced bubbles on echo integration surveys. *J. Acoust. Soc. Amer.*, **69**, 1653–1659, doi:10.1121/1.385943.

Deutschman, D., G. A. Bradshaw, W. M. Childress, K. Daly, D. Grunbaum, M. Pascual, N. Schumaker, and J. Wu, 1993: Mechanisms of patch formation. *Patch Dynamics*, S. A. Levin, T. M. Powell, and J. H. Steele, Eds., Springer Verlag, 184–209.

Dickey, T. D., E. C. Itsweire, M. Moline, and M. J. Perry, 2008: Introduction to the *Limnology and Oceanography* special issue on Autonomous and Lagrangian Platforms and Sensors (ALPS). *Limnol. Oceanogr.*, **53**, 2057–2061, doi:10.4319/lo.2008.53.5_part_2.2057.

Fernandes, P. G., A. S. Brierley, E. J. Simmonds, N. W. Millard, S. D. McPhail, F. Armstrong, P. Stevenson, and M. Squires, 2000: Oceanography: Fish do not avoid survey vessels. *Nature*, **404**, 35–36, doi:10.1038/35003648.

——, P. Stevenson, A. S. Brierley, F. Armstrong, and E. J. Simmonds, 2003: Autonomous underwater vehicles: Future platforms for fisheries acoustics. *ICES J. Mar. Sci.*, **60**, 684–691, doi:10.1016/S1054-3139(03)00038-9.

Foote, K. G., H. P. Knudsen, G. Vestnes, D. N. MacLennan, and E. J. Simmonds, 1987: Calibration of acoustic instruments for fish density estimation: A practical guide. ICES Cooperative Research Rep. 144, 71 pp.

George, R. A., L. Gee, A. W. Hill, J. A. Thomson, and P. Jeanjean, 2002: High-resolution AUV surveys of the eastern Sigsbee Escarpment. *Proc. Offshore Technology Conf.*, Houston, TX, Society of Petroleum Engineers, OTC 14139. [Available online at http://www.cctechnol.com/Files/Articles/171_0.pdf.]

Griffiths, G., and Coauthors, 2001: Standard and special: Sensors used during the Autosub Science Missions programme. *Proc. Symp. on Sensors and Autonomous Underwater Vehicles*, Miami Beach, FL, Autonomous Undersea Systems Institute, 16 pp.

Holliday, D. V., 1977: Extracting biophysical information from the acoustic signals of marine organisms. *Oceanic Sound Scattering Prediction*, N. R. Anderson, and B. J. Zahuranec, Eds., Plenum, 619–624.

Kloser, R., 1996: Improved precision of acoustic surveys of benthopelagic fish by means of a deep-towed transducer. *ICES J. Mar. Sci.*, **53**, 407–413, doi:10.1006/jmsc.1996.0057.

MacLennan, D. N., and D. V. Holliday, 1996: Fisheries and plankton acoustics: Past, present, and future. *ICES J. Mar. Sci.*, **53**, 513–516, doi:10.1006/jmsc.1996.0074.

McClatchie, S., R. E. Thorne, P. Grimes, and S. Hanchet, 2000: Ground truth and target identification for fisheries acoustics. *Fish. Res.*, **47**, 173–191, doi:10.1016/S0165-7836(00)00168-5.

Moline, M. A., and Coauthors, 2005: Remote environmental monitoring units: An autonomous vehicle for characterizing coastal environments. *J. Atmos. Oceanic Technol.*, **22**, 1797–1808, doi:10.1175/JTECH1809.1.

——, K. J. Benoit-Bird, I. C. Robbins, M. Schroth-Miller, C. M. Waluk, and B. Zelenke, 2010: Integrated measurements of acoustical and optical thin layers II: Horizontal length scales. *Cont. Shelf Res.*, **30**, 29–38, doi:10.1016/j.csr.2009.08.004.

Munk, W., and A. Baggeroer, 1994: The Heard Island papers: A contribution to global acoustics. *J. Acoust. Soc. Amer.*, **96**, 2327–2329, doi:10.1121/1.411316.

Niu, H., S. Adams, K. Lee, T. Husain, and N. Bose, 2009: Applications of autonomous underwater vehicles in offshore petroleum industry environmental effects monitoring. *J. Can. Pet. Technol.*, **48**, 12–16, doi:10.2118/09-05-12-GE.

Oliver, M. J., M. W. Breece, D. A. Fox, D. E. Haulsee, J. T. Kohut, J. Manderson, and T. Savoy, 2013: Shrinking the haystack: Using an AUV in an integrated ocean observatory to map Atlantic sturgeon in the coastal ocean. *Fisheries*, **38**, 210–216, doi:10.1080/03632415.2013.782861.

Panish, R., and M. Taylor, 2011: Achieving high navigation accuracy using inertial navigation systems in autonomous underwater vehicles. *Proc. IEEE Oceans 2011 Meeting*, Santander, Spain, IEEE, 7 pp., doi:10.1109/Oceans-Spain.2011.6003517.

Patel, R., N. O. Handegard, and O. R. Godo, 2004: Behaviour of herring (*Clupea harengus* L.) towards an approaching autonomous underwater vehicle. *ICES J. Mar. Sci.*, **61**, 1044–1049, doi:10.1016/j.icesjms.2004.07.002.

Robbins, I. C., G. J. Kirkpatrick, S. M. Blackwell, J. Hillier, C. A. Knight, and M. A. Moline, 2006: Improved monitoring of HABs using autonomous underwater vehicles (AUV). *Harmful Algae*, **5**, 749–761, doi:10.1016/j.hal.2006.03.005.

Scalabrin, C., C. Marfia, and J. Boucher, 2009: How much fish is hidden in the surface and bottom acoustic blind zones? *ICES J. Mar. Sci.*, **66**, 1355–1363, doi:10.1093/icesjms/fsp136.

Schmitt, R. W., and R. Petitt, 2006: A fast response, stable CTD for gliders and AUVs. *Proc. Oceans 2006*, Boston, MA, IEEE, 5 pp., doi:10.1109/OCEANS.2006.306907.

Stanton, T., 1982: Effects of transducer motion on echo-integration techniques. *J. Acoust. Soc. Amer.*, **72**, 947–949, doi:10.1121/1.388175.

Stokey, R. P., L. E. Freitag, and M. D. Grund, 2005a: A compact control language for AUV acoustic communication. *Oceans 2005—Europe*, Vol. 2, IEEE, 1113–1137.

——, and Coauthors, 2005b: Development of the REMUS 600 autonomous underwater vehicle. *Proceedings of the Oceans 2005 MTS/IEEE Conference and Exhibition*, Vol. 2, IEEE, 1301–1304.

Yuh, J., G. Marani, and D. R. Blidberg, 2011: Applications of marine robotic vehicles. *Intell. Serv. Rob.*, **4**, 221–231, doi:10.1007/s11370-011-0096-5.

Zawada, D. G., P. R. Thompson, and J. Butcher, 2008: A new towed platform for the unobtrusive surveying of benthic habitats and organisms. *Rev. Biol. Trop.*, **56** (Suppl.), 51–63, doi:10.15517/rbt.v56i0.5577.